



Evapotranspiration components determined by stable isotope, sap flow and eddy covariance techniques

D.G. Williams^{a,*}, W. Cable^b, K. Hultine^b, J.C.B. Hoedjes^c, E.A. Yopez^b,
V. Simonneaux^a, S. Er-Raki^d, G. Boulet^a, H.A.R. de Bruin^c, A. Chehbouni^a,
O.K. Hartogensis^c, F. Timouk^a

^a *Centre d'Etudes Spatiales de la Biosphère, Toulouse, France*

^b *School of Renewable Natural Resources, The University of Arizona, Tucson, USA*

^c *Meteorology and Air Quality Group, Wageningen University and Research Center, Wageningen, The Netherlands*

^d *Physics Department LMFE, Faculty of Sciences Semlalia, Marrakech, Morocco*

Received 21 September 2003; received in revised form 2 April 2004; accepted 16 April 2004

Abstract

Understanding and modeling water exchange in arid and semiarid ecosystems is complicated by the very heterogeneous distribution of vegetation and moisture inputs, and the difficulty of measuring and validating component fluxes at a common scale. We combined eddy covariance (EC), sap flow, and stable isotope techniques to investigate the responses of transpiration and soil evaporation to an irrigation event in an olive (*Olea europaea* L.) orchard in Marrakech, Morocco. The primary goal was to evaluate the usefulness of stable isotope measurements of water vapor in the turbulent boundary layer for partitioning evapotranspiration under such dynamic conditions. The concentration and deuterium isotope composition ($\delta^2\text{H}$) of water vapor was collected from different heights within the ecosystem boundary layer of the olive canopy before and over several days following a 100 mm surface irrigation. 'Keeling plots' (isotope turbulent mixing relationships) were generated from these data to estimate the fractions of evaporation and transpiration contributing to the total evapotranspiration (ET) flux. Transpiration accounted for 100% of total ET prior to irrigation, but only 69–86% of ET during peak midday fluxes over the 5-day period following irrigation. The rate of soil evaporation and plant transpiration at the stand level was calculated from eddy covariance measurements and the evaporation and transpiration fractions from isotope measurements. Soil evaporation rate was positively correlated with daily atmospheric vapor pressure deficit (D), but transpiration was not. Component fluxes estimated from the isotope technique were then compared to those obtained from scaled sap flow measurements. Sap flow in multiple-stemmed trees increased following the irrigation, but large single-stemmed trees did not. We matched the source area for eddy covariance estimates of total ET fluxes with scaled sap flow estimates developed for the different tree types. Soil evaporation was determined from the difference between total ET and the scaled sap flow. Ecosystem-level transpiration and soil evaporation estimated by the isotope approach were within 4 and 15% of those estimated by scaled sap flow, respectively.

* Corresponding author. Present address: Department of Renewable Resources, University of Wyoming, Dept. 3354, 1000 E University Ave., Laramie, WY 82071, USA. Tel.: +1 307 776 2263; fax: +1 307 766 6403.
E-mail address: dgw@uwyo.edu (D.G. Williams).

for periods of peak fluxes at midday. Our data illustrate the utility of the isotope ‘Keeling plot’ approach for partitioning ET at the ecosystem scale on short time steps and the importance of accurate spatial representation of scaled sap flow for comparison with eddy covariance measurements of ET.

© 2004 Elsevier B.V. All rights reserved.

Keywords: $\delta^2\text{H}$; Keeling plot; Transpiration; Soil evaporation; Water balance; Morocco; *Olea europaea*

1. Introduction

Evapotranspiration (ET) is an important component of ecosystem water balance and is strongly related to gross ecosystem production in terrestrial vegetation (Law et al., 2002). The correlation between ET and ecosystem production highlights the role of water as a principal limiting resource for plant photosynthetic metabolism. Ecosystem productivity is especially limited by water availability in arid and semiarid ecosystems (Noy-Meir, 1973), which are marked by highly variable moisture inputs in space and time (MacMahon and Schimpf, 1981). The frequently long periods of inactivity during dry periods in these environments are punctuated by active periods of water and carbon exchange following precipitation events. Accurate prediction of water exchange and ecosystem carbon metabolism in these dynamic resource environments requires an understanding of the factors driving the rates and timing of soil evaporation and plant transpiration at the ecosystem scale.

The contributions of soil evaporation and plant transpiration to total ecosystem ET in arid and semiarid environments are highly variable in space and time (Sammis and Gay, 1979; Evans et al., 1981; Smith et al., 1995; Kemp et al., 1997; Reynolds et al., 2000; Hutley et al., 2001; Ferretti et al., 2003). Prediction and modeling of evapotranspiration in these environments is complicated by the heterogeneous distribution of vegetation elements that often have different functional properties, and the difficulty of measuring components of water exchange at meaningful and comparable scales. These problems are especially acute during the very dynamic period following precipitation events when ET fluxes are highest and when soil and canopy conductances are changing rapidly (Huxman et al., 2004). Partitioning of the total evapotranspiration flux is important in these ecosystems because of the need to understand biotic and abiotic factors un-

derlying the efficiency with which water from pulsed inputs of rainfall is circulated through the transpiration pathway and thus contributes to photosynthetic gas exchange and productivity (Aguilar et al., 1996; Prince et al., 1998).

Evaporation and transpiration fluxes are separately represented in ecosystem water balance models (Paruelo and Sala, 1995; Reynolds et al., 2000), but are very difficult to measure independently at the ecosystem scale. Some surface-vegetation-atmosphere transfer (SVAT) models (e.g. SiSPAT, Braud et al., 1995; Boulet et al., 2000) operate at hourly or daily time steps, and thus are useful for investigating fluxes during the highly dynamic period following moisture pulses and extrapolating these fluxes to landscape and larger scales. However, ET parameterizations in SVAT models generally are validated at the ecosystem level using measurements of net fluxes taken at a single reference height above the vegetation (e.g. eddy covariance (EC) method). Soil evaporation and plant transpiration are often not independently verified with measurements at the same scale. Recently, measurements of the stable isotope composition of water vapor exchanged between vegetation and atmosphere have been used to trace the sources of ET at the ecosystem level allowing total ET fluxes to be partitioned into their component fluxes (Moreira et al., 1997; Harwood et al., 1999; Wang and Yakir, 2000; Yopez et al., 2003). When combined with eddy covariance measurements of ecosystem ET flux, the isotope partitioning approach becomes extremely powerful. Estimates of component fluxes from the isotope technique can be used to validate parameterizations in SVAT models. SVAT models then can be tested for their ability to predict how component fluxes and processes respond to changing environmental conditions after pulsed inputs of moisture in arid and semiarid environments. Water vapor for isotope measurements is typically collected at or near the same height that eddy covariance measurements

are made, but source area dimensions for the concentration measurements are larger than that for the fluxes (Schmid, 1994). Consequently, care should be taken when relating the eddy covariance and isotope techniques.

Evaporation from soil and transpiration from plants each contribute unique isotopic signals to water vapor within the ecosystem boundary layer. Water evaporated from the soil is depleted in the heavy isotopes (^2H , ^{18}O) compared to liquid water at the evaporating surface of the soil as a result of kinetic and equilibrium fractionations (Craig and Gordon, 1965; Allison et al., 1983). Although the water in leaves is enriched in the heavy isotopes during transpiration because of these same fractionations, at steady-state the water transpired from leaf surfaces is isotopically similar to that taken up by the plant's roots (Flanagan et al., 1991; Wang and Yakir, 1995). Since fractionation generally does not occur during uptake of water by roots (Dawson and Ehleringer, 1991; Thornburn et al., 1993), the isotopic composition of vapor derived from soil evaporation and plant transpiration is very different and easily distinguished.

Isotope ratios of the water vapor present in the planetary boundary layer (δ_{pbl}), within the turbulently mixed ecosystem boundary layer (δ_{ebl}), and that coming from evapotranspiration sources (δ_{ET}) can be represented by a mass balance mixing equation:

$$\delta_{\text{ebl}} = C_{\text{pbl}}(\delta_{\text{pbl}} - \delta_{\text{ET}}) \left(\frac{1}{C_{\text{ebl}}} \right) + \delta_{\text{ET}} \quad (1)$$

where C_{pbl} and C_{ebl} are the water vapor concentrations. This 'Keeling-type' relationship (Keeling, 1958; Yakir and Sternberg, 2000) is linear with a slope of $C_{\text{pbl}}(\delta_{\text{pbl}} - \delta_{\text{ET}})$ and an intercept (δ_{ET}) that represents the net isotopic contribution from the ET flux. Measurements of the concentration and isotopic composition of water vapor collected at different heights within the ecosystem boundary layer will provide data to fit the linear model. The fractional contribution of transpiration to the total ET fluxes (F_{T}) can be calculated from:

$$F_{\text{T}} = \frac{\delta_{\text{ET}} - \delta_{\text{E}}}{\delta_{\text{T}} - \delta_{\text{E}}} \quad (2)$$

where δ_{E} and δ_{T} are the isotopic compositions of soil evaporation and plant transpiration. Values for δ_{E} and

δ_{T} can be estimated from field sampling and modeling (Yakir and Sternberg, 2000).

Soil evaporation should comprise a significant fraction of the ET flux following input of water in semiarid and arid ecosystems (Paruelo and Sala, 1995). Soil evaporation rates initially are high following the wetting event, but decline rapidly as the soil surface dries (Ritchie, 1972). Transpiration may or may not change following inputs of water, depending on the rooting distribution of the dominant plants and response of leaf stomata to a change in soil water availability. The isotope technique recently was shown to be useful for partitioning ET within a semiarid ecosystem dominated by woody plants in the overstory and grasses in the understory (Yopez et al., 2003). However, the Keeling plot approach has not been employed to examine the short-term dynamics of evaporation and transpiration following a wetting event.

Sap flux techniques also are useful for partitioning total ET fluxes when combined with eddy covariance measurements (Hutley et al., 2001; Mackay et al., 2002), but scaling to the ecosystem level can be complicated by spatially and functionally heterogeneous vegetation (Schaeffer et al., 2000). Unique responses by different species or individuals to a wetting event and the poor representation of this variation within the footprint of the eddy covariance measurement can lead to significant error in partitioning estimates from sap flux. Scaling ecosystem-level transpiration from sap flux to the footprint of eddy covariance measurements presents unique challenges.

Here, we compare estimates of ET partitioning from eddy covariance and sap flux to that derived from stable isotope measurements of water vapor. These comparisons were made over several days following a large surface irrigation in an olive orchard in Marrakech, Morocco. Our goals were to: (1) test the utility of the Keeling plot method for partitioning ET fluxes over a dynamic wetting cycle in a semiarid environment; and (2) evaluate the consequences of plant functional heterogeneity for scaling sap flux to the ecosystem level. The study was part of a larger effort (project SUD-MED; <http://www.cesbio.ups-tlse.fr/cadrerech.htm>) to characterize the water and energy balance and hydrological resources in the Tensift region in southern Morocco.

2. Materials and methods

2.1. Site description

We conducted our study in the 275 ha Agdal olive (*Olea europaea* L.) orchard on the southern end of the ancient walled city of Marrakech, Morocco. Marrakech has a semiarid Mediterranean climate; 76% of the 253 mm average annual precipitation falls during winter and spring (November–April). Very little precipitation falls between May and October. Our study was conducted between October 27 and November 11 (DOY 300–315), 2002. No significant rainfall had been recorded at our study site for at least 100 days prior to initiation of our measurements.

The density of olive trees was $\sim 400 \text{ ha}^{-1}$ in the southeastern portion of the Agdal orchard where our study was conducted. Many of the trees at our study location were quite old, having been coppiced at least four times. Others had been recently planted in spaces where older trees had died. Thus, tree crown structure was somewhat variable across the study area; large, multi- and single-stemmed trees were interspersed with smaller and younger single-stemmed trees.

The Agdal olive orchard is periodically surface-irrigated by diverting flow from a large impoundment through a network of ditches. Water is diverted manually to every tree by manipulation of small earthen check dams. The $\sim 45 \text{ m}^2$ ground surface occupied by each tree is bordered by a small $\sim 30 \text{ cm}$ high earthen levy that retains the irrigation water, allowing precise application of irrigation water to every tree.

All understory plants were cleared from the study area by tilling prior to the start of measurements. Eddy covariance, micrometeorological, soil temperature, and sap flux measurements were continuously recorded over the 10-day study period. Isotope sampling took place on four dates; once prior to the large irrigation event, and three times following irrigation. Irrigation was applied on November 3 (DOY 307) to the section of the orchard containing our instrumentation. Irrigation completely wetted the entire soil surface of this 3 ha section with approximately 100 mm water.

2.2. Eddy covariance and micrometeorological measurements

Two 9.2 m tall instrument towers were erected in September 2002 in the Agdal orchard. One tower (south tower) was placed in the southeastern portion of the orchard near the center of the section that was irrigated on DOY 307. The second tower (north tower) was placed in the north-central portion of the orchard 3 km north of the first tower in an area that did not receive irrigation during the study period. Near-continuous measurements of water vapor, carbon dioxide, and sensible heat fluxes were recorded on each tower at 8.8 m height 2 m above the top of the olive canopy. A 3D sonic anemometer (CSAT3, Campbell Scientific, Logan, UT) on each tower measured the fluctuations in the wind velocity components and temperature. An open-path infrared gas analyzer (LI7500, LiCor, Lincoln, NE) measured concentrations of water vapor and carbon dioxide. The calm, prevailing winds were from the northeast to northwest during daytime periods of our study, providing a large and homogeneous fetch.

The wind speed and concentration measurements were made at 20 Hz on CR23X dataloggers (Campbell Scientific, Logan, UT) and on-site portable computers to enable the storage of large raw data files. Fluxes were later calculated off-line after performing coordinate rotations, correcting the sonic temperature for the lateral velocity and the presence of humidity, making frequency response corrections for slow apparatus and path length integration, and the inclusion of the mean vertical velocity according to Webb et al. (1980). Data from the eddy covariance system was processed using the software “ec-pack” developed by the Meteorology and Air Quality Group, Wageningen University. The software is available for download at <http://www.met.wau.nl/>.

Air temperature and humidity were measured at 8.8 and 3.7 m heights on the towers with Vaisala HMP45C probes. Total shortwave irradiance (S_i) was measured at 9.2 m height with a BF2 Delta T radiometer. Net radiation was measured with a Kipp and Zonen CNR1 net radiometer placed over the olive canopy at 8 m height. Soil temperature was recorded at 5 cm depth at two locations approximately 30 m from the towers. Three heat flux plates continuously monitored changes in soil heat storage at each of the two tower sites.

2.3. Sap flow measurements

We used a modified heat-pulse velocity technique (heat ratio method, HRM) to measure xylem sap flux on eight olive trees at the south tower (irrigation) site. The HRM employs temperature probes inserted into the active xylem at equal distances up- and downstream from a pulsed heat source. The difference in heat carried up- and downstream is proportional to the magnitude of sap flux (Burgess et al., 2001; Hultine et al., 2003). This technique was employed because of its precision at low sap velocities and because the heat-pulse velocity methods have been shown to be robust for olive (Fernández et al., 2001). Low transpiration rates were anticipated in the water-limited olives late in the dry season, before the irrigation input.

Sap flux sensors were installed on four large single-stemmed and four large multi-stemmed trees adjacent to the flux tower. Initial surveys revealed an aggregated, non-random distribution of these tree types within the potential flux source area of the tower. We did not measure sap flux in the young, single-stemmed trees that were sparsely scattered through the stand, but assumed that these trees would have similar sap flux rates and irrigation responses to the coppiced, multi-stemmed trees. Two sensors were installed on each of the eight trees. The HRM measurements were conducted every half-hour spanning DOY 303–313 using a datalogger control and measurement system (Hultine et al., 2003).

After correcting for wounding effect (Burgess et al., 2001), heat-pulse velocity was converted to sap velocity according to Barrett et al. (1995) using $1200 \text{ J kg}^{-1} \text{ }^\circ\text{C}^{-1}$ for the specific heat of dry wood, $4182 \text{ J kg}^{-1} \text{ }^\circ\text{C}^{-1}$ for the specific heat of xylem sap (assumed to equal that of water at 20°C) and $1.0 \times 10^3 \text{ kg m}^{-3}$ for the density of sap (assumed to equal that of water). Wood density and moisture content were measured on 12 cores from single-stemmed trees and 12 cores from multi-stemmed trees. We validated zero flow in situ at the end of the 10-day measurement period by drilling 2 cm diameter holes ~ 10 cm up- and downstream from the probe to completely interrupt flow in the vicinity of the sensors. The holes were then sealed with silicon to prevent desiccation during the zeroing measurements. Spac-

ing error between probes was calculated according to Burgess et al. (1998).

Volumetric sap flow (L h^{-1}) was calculated from sap velocity with measurements of the active sapwood area of trees fitted with HRM probes. Sapwood area was calculated first by subtracting the bark thickness from the total radius of the stem. The heartwood depth, visually identified by its dark color on core samples, was used to calculate heartwood area. This was then subtracted from total wood area to estimate sapwood area for each tree. The sapwood area was then divided into concentric bands coinciding with the depth into the sapwood of each thermocouple junction within the probes (10, 20, and 30 mm). A linear decay function was used to estimate sap velocity within the active xylem at depths beyond the insertion of the probe. Thus, estimates of sap flow were adjusted by the percent of conducting sapwood of each band.

Scaling of sap flow to the eddy covariance source area was facilitated with a detailed survey of average per tree sapwood area for the three tree classes in the stand. Thirty single-stemmed, 16 multi-stemmed and 10 young trees were randomly selected from within a $200 \text{ m} \times 200 \text{ m}$ plot using the tower as the center position. Each stem was measured for diameter at 1 m above ground surface, bark thickness, sapwood depth, and per cent damage to the stem. These data were used to estimate sapwood area using the above procedure. Additionally, every tree (965 total) within the $200 \text{ m} \times 200 \text{ m}$ plot was assigned to one of the three tree classes. A portion of the plot extended beyond the northern boundary of the section irrigated on DOY 307. Trees that fell within this non-irrigated section were noted. Volumetric sap flow was scaled to transpiration on a ground area basis (mm h^{-1} or mm d^{-1}) from measurements of the average ground area domain (41.9 to 46.0 m^2 per tree) occupied by each tree type within the potential eddy covariance flux source area.

2.4. Evapotranspiration partitioning from sap flow and eddy covariance

We assumed that differences between the total ecosystem evapotranspiration estimated by eddy covariance and ecosystem transpiration estimated from

scaled sap flow before irrigation were due to error in sap flow scaling. Since soil evaporation during this pre-irrigation period was negligible (the soil was dry to 30 cm depth prior to irrigation), the ET flux measured by EC was used to calibrate the scaled sap flow measurements for estimating stand transpiration. After calibrating the scaled sap flow estimates of transpiration to the EC measurements for this pre-irrigation period, differences between scaled sap flow and ET from eddy covariance after irrigation were presumed to reflect the contribution of soil evaporation. To compare sapflow estimates of transpiration on a per tree basis (as described in Section 2.3) to the evapotranspiration estimates from EC, we calculated the EC flux footprint (i.e. the relative contribution of each unit element of the upwind surface area to the measured vertical flux). Also, to ensure that we scaled sap flux to the corresponding flux source area measured by the EC system, we spatialized the tree distribution according to the above mentioned tree-classification within the EC source area.

The EC flux source area for each interval was calculated using the analytical footprint model proposed by Horst and Weil (1992, 1994). The flux footprint f , or the contribution per unit surface flux of each unit element of the upwind surface area to a measured vertical flux, is related to the vertical flux measured at height z_m , $F(x, y, z = z_m)$, and to the spatial distribution of surface fluxes, $F(x, y, z = 0) \equiv F_0(x, y)$, i.e.

$$F(x, y, z_m) = \int_{-\infty}^{\infty} \int_{-\infty}^x F_0(x', y') f(x - x', y - y', z_m) dx' dy' \quad (3)$$

(Horst and Weil, 1992). The source area arises from the integration of the footprint function. In this study we calculated the crosswind-integrated footprint function using the model of Horst and Weil (1994):

$$\bar{f}^y(x, z_m) \cong \frac{d\bar{z}}{dx} \frac{z_m}{\bar{z}^2} \frac{\bar{u}(z_m)}{\bar{u}(c\bar{z})} A e^{-(z_m/b\bar{z})^r} \quad (4)$$

where \bar{z} is the mean plume height for diffusion from a surface source and $\bar{u}(z)$ the mean wind speed profile. The variables A , b and c are gamma functions of shape parameter r . We have assumed that $U(x) = \bar{u}(c\bar{z})$, and that the violation of the Monin–Obukhov similarity theory is small (Horst, 1999; Meijninger et al., 2002).

In order to spatialize the surface contributions to evapotranspiration, the trees within the 200 m × 200 m

plot surrounding the eddy-covariance tower (965 trees in total) were georeferenced using a high resolution satellite image of the orchard, and every tree was assigned to one of the three tree classes. A detailed land-cover layer was thus obtained. Overlaying this layer with the calculated EC flux source area (i.e. overlaying the land cover layer with a “ponderation field” for surface contributions) allowed us to obtain the relative contributions for each of the tree classes (either single-stemmed, multi-stemmed, young tree or missing tree; irrigated or non-irrigated) for each interval. Combining these relative contributions and the sap flow estimated transpiration of each tree-type, the total footprint-integrated transpiration within the EC flux source area was calculated.

2.5. Isotope sampling

Water vapor was collected on four dates (DOY 303, 308, 310, and 313) at the south (irrigated) site with an automated cryogenic trapping system (Yepez et al., 2003). Water vapor was collected from five heights within the ecosystem boundary layer (8.9, 6.4, 3.7, 1.2 and 0.1 m above ground surface) by drawing air through low-absorption tubing attached to the eddy covariance tower. Air was pumped through a network of solenoid switching valves that every 90 s routed the air from each height through a hygrometer (OEM-2010, Yankee Environmental Systems, MA, USA) to record dew point temperature. From each height, air continuously circulated through glass vapor traps (modified from Helliker et al., 2002) immersed in an alcohol bath. The alcohol was kept at -80°C by periodically adding liquid nitrogen. Samples from the five heights were collected during three 30 min periods between 10:00 and 12:30 h and between 14:00 and 16:30 h on each sampling day (30 samples total on each day). Sample traps were removed from the alcohol after 30 min of continuous trapping and then sealed with a rubber stopper and Parafilm. Water was quantitatively transferred from the vapor traps within 48 h after collection to flame-sealed 6 mL diameter Pyrex tubes by cryogenic vacuum distillation (Ehleringer and Osmond, 1989).

Plant and soil samples were collected at midday (13:00–14:00 h) on all sampling days to estimate the $\delta^2\text{H}$ value of soil evaporation (δ_E) and plant transpiration (δ_T). It was assumed that transpiration of olive

trees was at isotopic steady-state, such that the $\delta^2\text{H}$ value of non-evaporated twig xylem water would be representative of that of transpiration vapor during the sample collection periods (Yakir and Sternberg, 2000). Soil and olive twig samples ($n = 4\text{--}6$ per sample day) were collected near the south tower. Soil samples were collected from 20 to 30 cm depth (the shallowest moist soil layer) on DOY 303 prior to irrigation and from the moist soil surface (0–2 cm depth) on sampling days after irrigation. Twig and soil samples were placed into screw-cap glass vials, sealed with Parafilm, and extracted by cryogenic vacuum distillation into flame-sealed Pyrex tubes within a few days of collection. A single sample of the irrigation water was collected on DOY 307.

2.6. $\delta^2\text{H}$ analysis

$\delta^2\text{H}$ analysis was performed at the University of Arizona Laboratory of Isotope Geochemistry on a dual-inlet stable isotope ratio mass spectrometer (Delta S, Finnigan MAT, San Jose, CA, USA), except for vapor samples collected on DOY 313. Small ($3\ \mu\text{L}$) water subsamples were injected into a reaction furnace (HDevice, Finnigan MAT, San Jose, CA, USA) in the presence of chromium at $1025\ ^\circ\text{C}$ to produce diatomic hydrogen (Nelson and Dettman, 2001). The hydrogen was transferred on-line into the sample bellows on the mass spectrometer for analysis. The standard deviation for repeated analysis of calibrated working standards with this method was 0.8%. Vapor samples from DOY 313 were analyzed by pyrolysis with a continuous flow method on a Finnigan MAT Delta^{plus} stable isotope mass spectrometer (San Jose, CA, USA) coupled with a thermal combustion elemental analyzer (Finnigan MAT TC-EA, San Jose, CA, USA) that combusted samples at $1380\ ^\circ\text{C}$. Samples then flowed at $40\ ^\circ\text{C}$ and $50\ \text{ml}\ \text{min}^{-1}$ from a GC column packed with $5\ \text{\AA}$ molecular sieve to the mass spectrometer. The repeated measurements of known standards had a standard deviation for $\delta^2\text{H}$ of 2%. All $\delta^2\text{H}$ values are reported relative to V-SMOW.

2.7. Evapotranspiration partitioning from isotopes

The $\delta^2\text{H}$ value of the ET flux (δ_{ET} ; Eq. (2)) was estimated from the y-axis intercept of the linear regres-

sion of δ_{ebl} (the $\delta^2\text{H}$ value of water vapor) on the reciprocal of water vapor concentration (Eq. (1)) for the samples collected within the morning or afternoon periods on each of the four sampling days. The water vapor concentration ($\text{mmol}\ \text{mol}^{-1}$) was calculated from measurements of dew-point temperature (see Section 2.4) and total atmospheric pressure at the south tower site. The spreadsheet model Isoerror (version 1.04; Phillips and Gregg, 2001) was used to estimate the fractions and variance components of transpiration and soil evaporation sources contributing to the total ET flux. The mean $\delta^2\text{H}$ value of olive-twig xylem water was used for the transpiration isotope value (δ_{T}) in the isotope mixing model. The isotope value of soil evaporation (δ_{E}) was estimated from the Craig–Gordon evaporation model (Craig and Gordon, 1965) using measurements of soil temperature, humidity, and the $\delta^2\text{H}$ values of soil water and water vapor near the soil surface. The temperature-dependent equilibrium

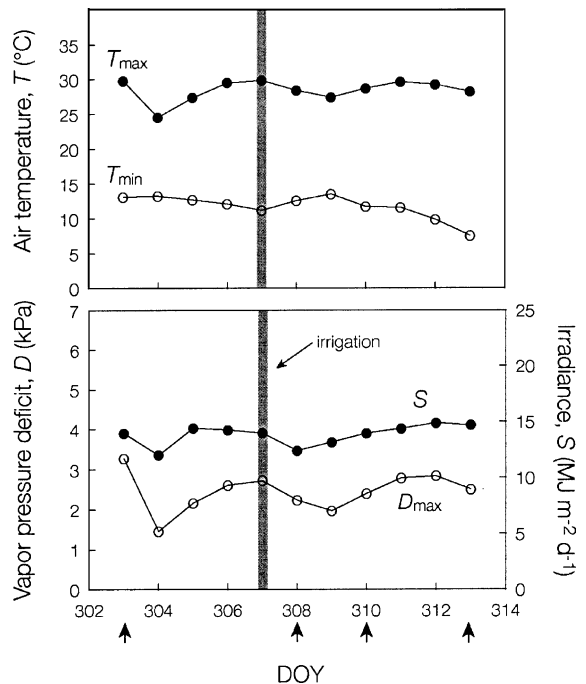


Fig. 1. Daily trends in environmental conditions at the Agdal south tower site during the 10-day study period. Conditions were measured near the top of the 9 m tower at the site, above the olive canopy (see Section 2.2). Arrows along the x-axis show the dates on which stable isotopes were sampled. The vertical bar shows the date of irrigation.

fractionation factor for the liquid-vapor phase change was calculated from Majoube (1971). The kinetic fractionation was assumed to be high (26‰) for the period prior to irrigation (diffusive transport through dry soil), and low (13‰) after irrigation (turbulent transport from wet soil surface) (Merlivat, 1978).

3. Results and discussion

Accurate measurement of the component fluxes of ET on a scale useful for integration with eddy covariance and remote sensing is necessary for the development and validation of modeling and observation tools that can be used to monitor and predict the dynamic responses of water-limited ecosystems to rainfall variability. Our study took place over a 10-day period at the end of the dry season in an olive orchard in southern Morocco. Meteorological

conditions were fairly stable over the study period; air temperature, solar radiation, and vapor pressure deficit were high, especially after irrigation, providing optimal conditions for flux and stable isotope measurements (Fig. 1). Vapor pressure deficit increased over the last several measurement periods providing an opportunity to investigate responses of vegetation and soil components to variable ET demand by the atmosphere. Isotope sampling took place under calm, cloudless conditions. However, afternoon sampling (14:30–16:30 h) took place under changing conditions as solar irradiance and air temperature declined at the end of the solar period (Fig. 2).

3.1. Evapotranspiration estimated by eddy covariance

Sap flow and isotope measurements were carried out within the potential flux source area measured by an eddy covariance system installed on a 9.2 m tower

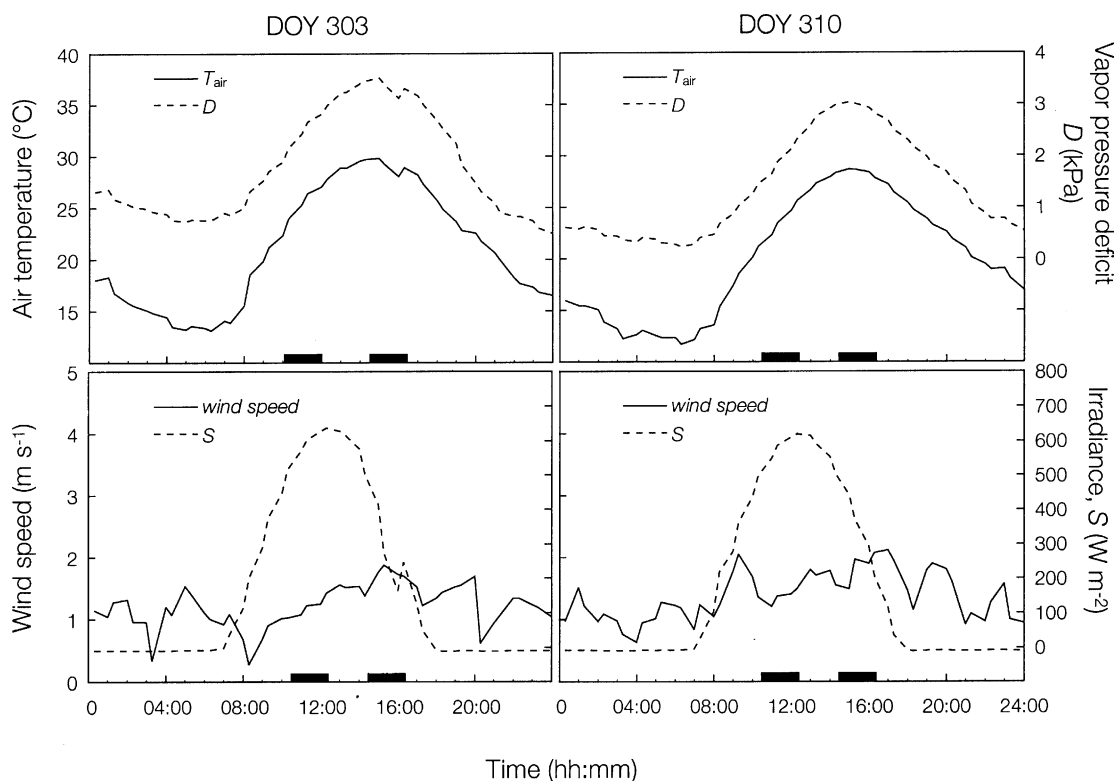


Fig. 2. Example of diurnal trends in environmental conditions on 2 days during the study. Horizontal bars above x-axis show the time intervals during which atmospheric water vapor was collected for stable isotope analysis.

in the southern portion of the Agdal olive orchard. The validity of eddy covariance measurements at this site was tested by evaluating how well the available energy (i.e. net radiation, R_n , minus ground heat flux, G) was balanced by the sum of the turbulent fluxes (i.e. the sum of the latent, λE , and sensible, H , heat fluxes). Closure of the energy balance ($R_n - G = \lambda E + H$) depends on the validity of the eddy covariance measurements and the ability to quantify the available energy within the flux source area. The closure of the energy balance was acceptable (slope = 0.74, $r^2 = 0.94$) for this site over the 10-day measurement period (Fig. 3). Energy storage within the olive tree biomass and in the air column beneath the R_n measurement are not included in this simple analysis. Energy storage within the biomass may account for as much as 10% of the available energy in such ecosystems (Scott et al., 2003). Soil heat flux plates used to estimate G were concentrated in a shaded area on the north side of a large olive tree at the south tower site. We are not confident that this location accurately represented G for the flux source area across the orchard as many locations were exposed to higher direct solar radiation than the area chosen for soil heat flux measurements. Such exposed locations likely experience much higher positive G during the day and higher negative G during the night compared to that in shady locations. These differences easily could account for

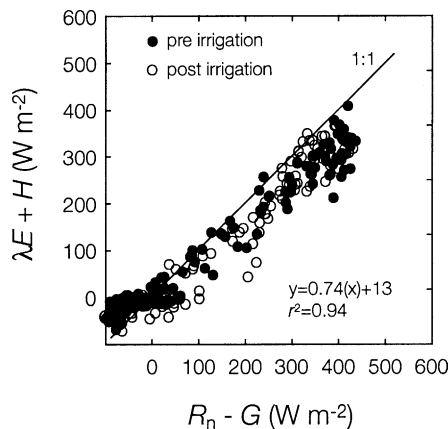


Fig. 3. Energy balance closure for the Agdal south tower site. Data are paired 30 min averages collected before the irrigation on DOY 303–306 (●) and after irrigation on DOY 308–313 (○). The 1:1 line is provided as is the regression equation and coefficient of determination for the best-fit line through the data.

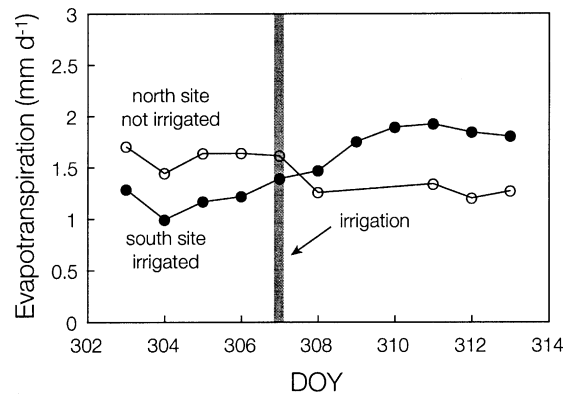


Fig. 4. Comparison of daily total evapotranspiration observed at the Agdal North (not irrigated) and Agdal south (irrigated) sites. The vertical line shows the date on which irrigation was applied.

the apparent lack of energy closure observed. Despite these minor concerns about energy closure, we were confident that the eddy covariance measurements accurately estimated ET.

The 100 mm surface irrigation event on DOY 307 enhanced ET by 54% over that in the few days before irrigation (Fig. 4). Compared to daily total ET recorded at the north tower site (not irrigated), the irrigated south site showed a pronounced upward shift in ET following irrigation that was apparently not driven solely by changing meteorological conditions (Fig. 1). The initially higher ET rates at the north site compared to that at the south site was likely due to the more recent irrigation at that site prior to the start of our measurements on DOY 303; soil was still visibly moist just beneath the surface at the north site on DOY 303. The upper soil profile was quite dry at the south site prior to irrigation.

3.2. Partitioning of ET from scaled sap flow measurements

Our goal was to investigate the component contributions to enhanced ET rates observed following irrigation at the south tower site. The difference between total ET and ecosystem-level transpiration estimated from scaled sap flow measurements offers one approach to partitioning these fluxes. This method is widely applied (Wilson et al., 2001), but often does not provide satisfactory results. Dominant components of natural vegetation (i.e. species, functional

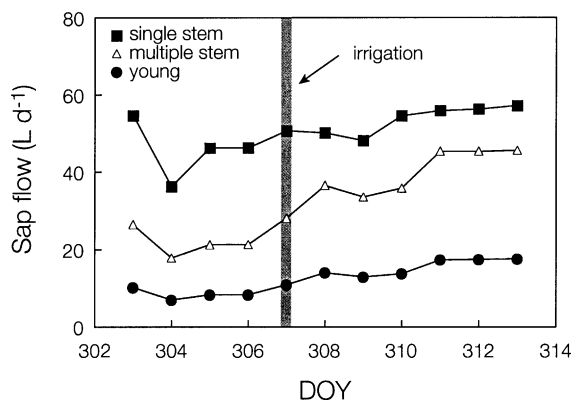


Fig. 5. Average daily sap flow per tree for the three tree classes at the Agdal south tower site. Values were calculated from average sap velocity recorded by the HRM sensors and the average sapwood area measured on a subset of trees at the site. Sap velocity measured for multiple stemmed trees was used to estimate sap flow in the young single-stemmed trees. The vertical line shows the date on which irrigation was applied.

types) are heterogeneously distributed within ecosystems and among landscape units and often have unique responses to wetting events (Williams and Ehleringer, 2000). To be successful, partitioning of ET fluxes from scaled sap flow must account for this heterogeneity through distributed sampling. The flux source area measured by eddy covariance can change rapidly depending on wind speed and direction and can frustrate attempts to match scaled sap flow to eddy covariance measurements. This is arguably less of a problem in a tree orchard where cultivation has led to a structurally and functionally homogenous vegetation cover. However, sap flow in the multi- and single-stemmed olive trees in this study responded very differently to irrigation (Fig. 5). Average daily sap flow in the large single-stemmed trees increased only slightly (17%; from 49.5 to 53.8 L d⁻¹) following the irrigation, whereas the average sap flow of multi-stemmed trees increased by 86% (21.8 to 40.4 L d⁻¹). Multi-stemmed trees occur on less favorable micro-sites within the orchard and experience greater levels of water stress, and thus respond more to the periodic irrigations. In fact, these trees were coppiced because they were less productive.

We modeled the source flux area measured from the tower and used this to scale tree sap flow to the ecosystem level based on a geographically

referenced classification of the olive tree types (Fig. 6). Sap flux measurements were not made on the young single-stemmed trees because they represented only 9.4% of all trees in the stand. The large single-stemmed trees accounted for 77.3% and multi-stemmed trees accounted for 13.3% of trees in the stand. For the purposes of scaling transpiration to the stand level, we assumed that sap flux in the young single-stemmed trees was the same as that in multi-stemmed trees. Although we anticipated in our sap flow sampling design that prevailing winds and the flux source area would include a large cluster of multi-stemmed trees situated to the west-northwest of the eddy covariance tower (Fig. 6), the winds were predominantly from the northeast over the study period where very few multi-stemmed trees were found. By super-imposing the calculated flux footprint over a geographically referenced tree classification, we determined that on average only 1.8% of the flux source area during daytime periods was occupied by multi-stemmed trees. Large single-stemmed trees occupied 88.7% of the flux source area, and the much smaller young single-stemmed trees occupied 7.3% of the flux source area. Since whole-tree sap flow was low in the young single-stemmed trees (Fig. 5), their contribution to stand transpiration was minimal. Simple scaling of sap flow from the absolute proportions of each tree type from the initial surveys would have led to considerable error in partitioning estimates. Accounting for spatial and functional heterogeneity in tree sap flow, especially when integrating with eddy flux measurements is clearly important, even in relatively homogeneous tree orchards.

We assumed that differences between sap flow scaled to the eddy covariance footprint and the eddy covariance estimates of ET would reflect the contribution of soil evaporation. This difference should be negligible when the soil surface is dry, as was the case prior to irrigation (DOYs 303–306) at the south tower site. However, our scaled sap flow tended to underestimate ET during this period by about 24% (Fig. 7). This error is likely due to either: (1) underestimation of wounding damage (Swanson and Whitfield, 1981); (2) a failure to capture sap flux in the most active region of the xylem that is generally located near the cambium (Swanson, 1994); or (3) underestimation of sap flux at depths beyond which our sensors were

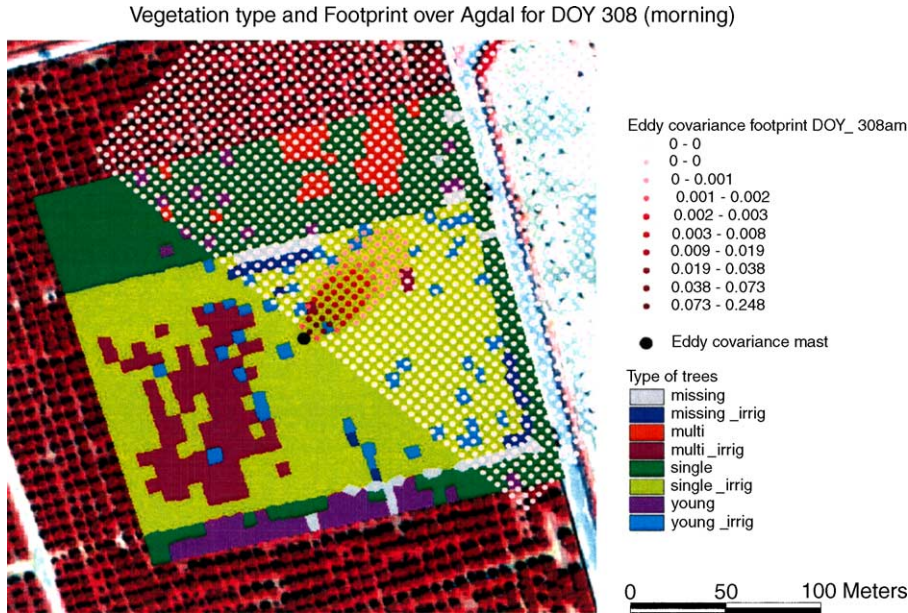


Fig. 6. Example from the Agdal south site showing the spatialized tree classification used for scaling sap flow and integrating the scaled sap flow estimates with the ET source area footprint model. Data are for DOY 308, averaged from 10:00 to 12:30h. Each spatial element of the footprint model is assigned a proportion of the total ET flux from the up-wind field. Each tree element is assigned to the following classification categories: single-stemmed, “single”; multi-stemmed, “multi”; young tree, “young”; or missing tree, “missing”; irrigated, “irrig” or non-irrigated (no designation).

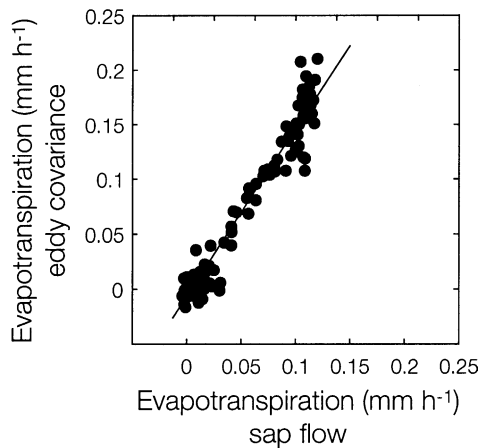


Fig. 7. Correlation between sap flow measurements scaled to the eddy covariance flux footprint and the eddy covariance ET flux for DOY 303–306, before irrigation. Soil surface conditions were very dry during this period. This relationship was used to calibrate the scaled sap flow measurements for extrapolation to post-irrigation transpiration.

designed to measure (in this case, 30 mm, [Fernández et al., 2001](#)).

The consistent error associated with the scaled sap flow measurements was overcome for the purposes of ET partitioning by using the pre-irrigation period to calibrate sap flow to the eddy covariance measurements. We recalculated all the scaled sap flow data with a regression model relating paired sap flow and eddy covariance estimates of ET from each 30 min interval between DOY 303 and 306 ([Fig. 5](#)). The linear regression model ($\text{Transpiration} = 1.56 * [\text{scaled sap flow}] - 0.009$) was statistically significant ($P < 0.001$) and accounted for more than 95% of the total variance ($r^2 = 0.954$). Prevailing wind speed and direction was similar between the calibration period before irrigation and during the period after irrigation (data not shown), thus we were confident that this model was valid for the post-irrigation period. Further, over the entire measurement period no less than 85% of the flux was derived from areas occupied by single-stemmed trees within the irrigated area and no more than 2% of the flux was derived

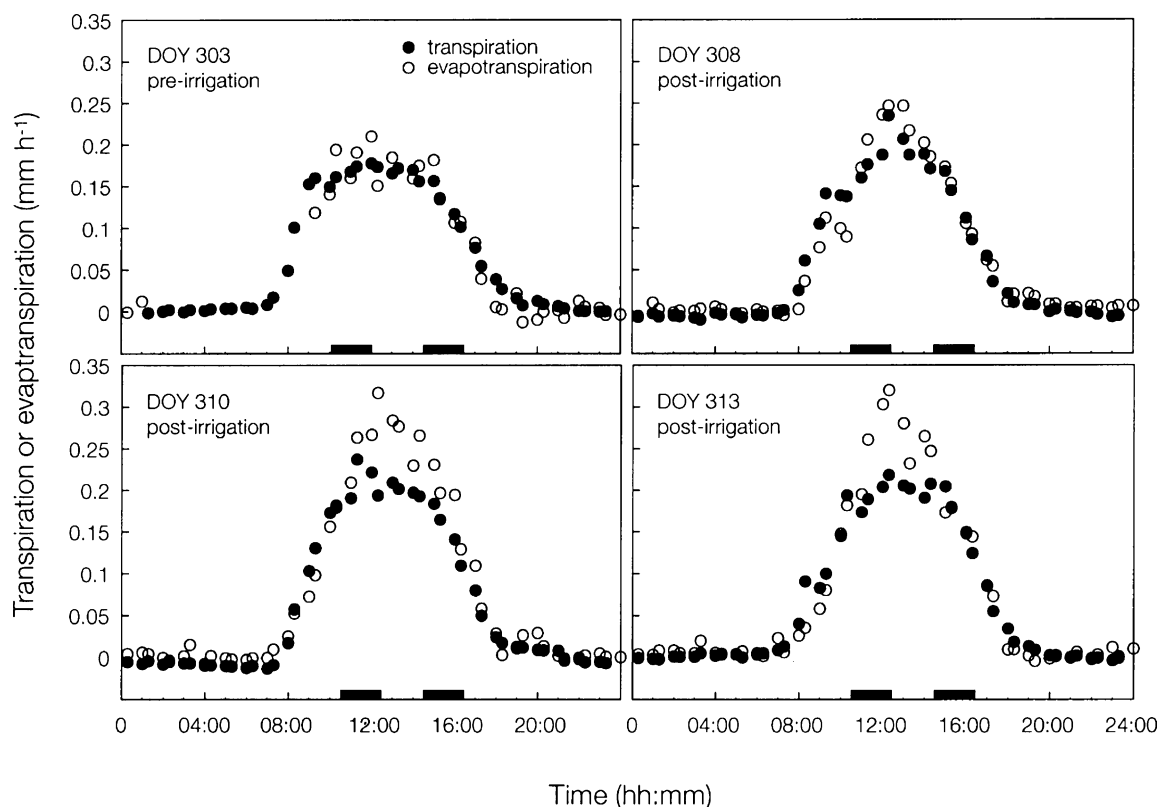


Fig. 8. Daily course of scaled transpiration from calibrated sap flow and evapotranspiration measured by the eddy covariance system at the Agdal south site. Horizontal bars above x-axis show the time intervals during which atmospheric vapor was sampled for isotope analysis.

from the non-irrigated area. Thus, the shifts in wind direction and speed over the 10-day measurement period did not have much bearing on the type of vegetation included within the source flux area, adding further validity to the pre-irrigation calibration and application. Total ET flux recorded by the eddy covariance system was higher than the adjusted, scaled values of olive transpiration on days 308, 310, and 313 – the days on which stable isotope measurements were taken after irrigation (Fig. 8). The differences reflect the significant contribution of soil evaporation to total ET within the flux footprint of the eddy covariance measurements. The soil surface remained very moist through the last sampling day (DOY 313). We likely did not capture during this period the second phase of soil drying when evaporation becomes limited by surface resistance (Ritchie, 1972).

3.3. Partitioning of ET from δ^2H of atmospheric water vapor

Large gradients in atmospheric moisture content and isotopic composition through the profile of the ecosystem boundary layer were observed on all the sampling dates except DOY 303, the sampling date prior to irrigation. Linear regressions were fitted to morning and afternoon data to estimate δ_{ET} , the isotopic composition of the ET flux, separately for these periods, except from DOY 303 for which morning and afternoon data were combined for a single estimate of δ_{ET} (Fig. 9). The y-intercepts for these best-fit regressions estimate δ_{ET} (Table 1). The value for δ_{ET} was more negative on the days following irrigation than prior to irrigation, likely reflecting the input of water vapor lost from the soil surface, which carried a very depleted isotope signal (Table 2).

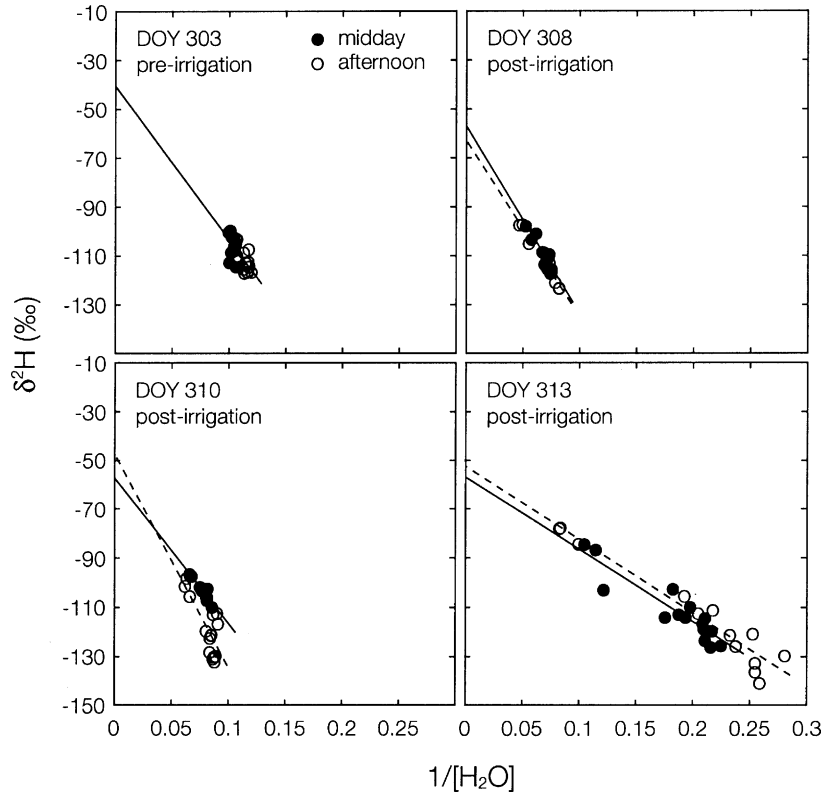


Fig. 9. Deuterium isotope ($\delta^2\text{H}$) mixing relationships ('Keeling plots') generated for each sampling period (midday = 10:30–12:30 h; afternoon = 14:30–16:30 h) on DOY 303, 308, 310, and 313. Lines represent best-fit regressions for each period. Data for midday and afternoon were combined for the regression analysis on DOY 303.

Table 1
Summary of linear regression analyses from Keeling plots of atmospheric water vapor (Eq. (1) in text)

Sampling period	<i>N</i>	Slope	y-Intercept	<i>r</i> ²	Significance of <i>F</i> statistic
DOY 303					
10:00–12:00 h + 14:30–16:30 h	27	−630 (118)	−40 (13)	0.53	<i>P</i> < 0.001
DOY 308					
10:30–12:30 h	12	−771 (115)	−57 (8)	0.82	<i>P</i> < 0.001
14:30–16:30 h	15	−723 (42)	−63 (3)	0.95	<i>P</i> < 0.001
DOY 310					
10:30–12:30 h	14	−594 (57)	−57 (4)	0.90	<i>P</i> < 0.001
14:30–16:30 h	15	−869 (198)	−48 (16)	0.56	<i>P</i> < 0.001
DOY 313					
10:30–12:30 h	15	−295 (35)	−57 (7)	0.85	<i>P</i> < 0.001
14:30–16:30 h	13	−300 (24)	−52 (5)	0.93	<i>P</i> < 0.001

Values in parentheses represent 1 S.E. of the parameter estimate.

Table 2

Estimates of the $\delta^2\text{H}$ value of evapotranspiration (δ_{ET}) from Table 1 and the isotope values of plant transpiration (δ_{T}) and soil evaporation (δ_{E}) sources for each sampling period

Sampling period	δ_{T}	δ_{E}	δ_{ET}	F_{T}	F_{E}
DOY 303					
10:00–12:00 h + 14:30–16:30 h	–44 (2)	–131 (2)	–40 (13)	1.05 (0.15)	–0.05 (0.15)
DOY 308					
10:30–12:30 h	–46 (1)	–123 (5)	–57 (8)	0.86 (0.10)	0.14 (0.10)
14:30–16:30 h		–120 (5)	–63 (3)	0.77 (0.04)	0.23 (0.04)
DOY 310					
10:30–12:30 h	–46 (1)	–106 (4)	–57 (4)	0.82 (0.07)	0.18 (0.07)
14:30–16:30 h		–120 (4)	–48 (16)	0.97 (0.22)	0.03 (0.22)
DOY 313					
10:30–12:30 h	–41 (1)	–93 (2)	–57 (7)	0.69 (0.13)	0.31 (0.13)
14:30–16:30 h		–86 (2)	–52 (5)	0.75 (0.11)	0.25 (0.11)

Also shown are the estimated fractions of evapotranspiration from tree transpiration (F_{T}) and soil evaporation (F_{E}). Values in parentheses are 1 S.E. of the means. Data from midday and afternoon sampling on DOY 303 were combined.

The $\delta^2\text{H}$ value of the irrigation water applied on DOY 307 was -30‰ . Interestingly, the $\delta^2\text{H}$ value of olive twig water remained near -45‰ throughout the study period until DOY 313 when average twig $\delta^2\text{H}$ values increased to -41‰ (Table 2). The increase in $\delta^2\text{H}$ values 6 days after the irrigation likely reflects uptake of irrigation water by the trees. Unfortunately, we did not sample intensively enough within single- and multi-stemmed trees to distinguish differences between the two types in the timing our quantity of uptake of the irrigation water. However, because sap flow rates in the multi-stemmed trees responded very significantly to the irrigation, even by the 3rd day after irrigation, water stress in these trees likely was ameliorated by the irrigation.

The $\delta^2\text{H}$ values estimated for olive transpiration and soil evaporation differed from each other by 45–87‰ over the 10 days sampling period, providing very distinct signals for partitioning analysis (Table 2). The fraction of total ET from soil evaporation (F_{E}) ranged from 0 on DOY 303 prior to irrigation to as high as 0.31 at midday on DOY 313. Although midday F_{E} increased from DOY 308 to 313, F_{E} was quite variable over these days in the late afternoon sampling periods. The high variance for the estimated fractions on the afternoon of DOY 310 indicates that the technique was flawed during this sampling period. The rapidly changing environmental conditions and total ET fluxes during this late afternoon period (Fig. 2) may have led to unstable proportional fluxes from trees

and soil over the 2-h sampling period and/or isotopic non-steady-state fluxes from trees (Harwood et al., 1999). Either mechanism could produce high variance in Keeling plot data or inaccurate or non-interpretible estimates of $\delta^2\text{H}$ values for ecosystem ET. Regression analysis using only the first of the three sets of five atmospheric vapor samples (14:30–15:00 h) produced an estimate of -58‰ for the $\delta^2\text{H}$ value of ecosystem ET, which contrasted sharply with that estimated from all three sample sets (-48‰) during this period. For these reasons, we were not confident with the isotope partitioning results from the afternoon periods.

The principal assumptions for the valid application of the Keeling plot method for partitioning ET from measurements of stable isotope ratios of atmospheric moisture, plants, and soils in this study are that: (1) plants are transpiring at isotopic steady-state, such that vapor transpired from leaves has the same stable isotope value as that sampled from twigs; (2) there is no loss of water vapor other than that lost from turbulent mixing with the atmosphere (e.g. no condensation); (3) there are no more than two sources for the evapotranspired water vapor; and (4) the relative contributions of the two sources does not change within an analysis period (Yakir and Sternberg, 2000). Assumptions 2 and 3 are easily met in the simple, two-layered olive ecosystem. The warm, dry conditions precluded any possibility of condensation during our measurements and all understory plants were removed prior to the study such that the soil was completely bare. We

assumed that the short intervals for morning and afternoon measurements (~ 2 h) was insufficient time to allow large shifts in the proportional fluxes from transpiration and soil evaporation. We did not directly test the assumption of isotopic steady-state, however, because of the large differences in the isotope values of modeled soil evaporation flux (δ_E) and twig water (δ_T), we assumed that deviations from isotopic steady-state transpiration would not greatly compromise accuracy in our partitioning estimates. The most unfavorable conditions for applying this approach were clearly during the afternoon sampling periods, when solar irradiance (Fig. 2), olive transpiration, and ET fluxes were declining rapidly (Fig. 8).

3.4. Technique comparison

Partitioning total ET into its components at the ecosystem or larger scale requires integration of several measurement techniques. Often these techniques require measurements that differ greatly in spatial or temporal scale (Grelle et al., 1997; Wilson et al., 2001). Tree sap flow and stable isotope estimates of component ET fluxes are derived from measurements representing very different spatial scales. Sap flow is typically carried out on just a subset of trees within the stand, and it is assumed that these trees capture the variance and mean response of all trees within the footprint of the eddy covariance flux measurements. This is a reasonable assumption for a relatively homogeneous agricultural ecosystem, but we found it necessary to account for tree-to-tree variation in sap flow responses in the Agdal olive orchard. Confidence in the component ET estimates was improved by scaling tree sap flow responses to the flux source area of the eddy covariance measurements. Careful evaluation of flux source area is even more essential in natural vegetation where heterogeneity in species composition and stand structure precludes accurate representation of ET components at a large scale (Grelle et al., 1997; Mackay et al., 2002). Still, this technique depends on adequate sampling of trees within each class and validity of the eddy flux source area modeling (Moncrieff et al., 2000; Mackay et al., 2002). Another concern with sap flow measurements is that tree capacitance can lead to temporal lags between rates of sap movement in the base where measurements are made and evaporation from leaf surfaces (Goldstein

et al., 1998). We saw little evidence of a lag between sap flow and ET in olive.

The isotope technique arguably has fewer constraints with respect to spatial and temporal scale when partitioning fluxes measured by eddy covariance. Isotope samples are collected within the ecosystem boundary layer, including the constant flux zone where eddy covariance sensors are deployed. Thus, the footprint for the atmospheric vapor samples is somewhat similar to that for the eddy covariance measurements (but see Rannik et al., 2000). Although we collected some samples for isotope analysis from near the ground surface, the Keeling plots were linear (Fig. 9) with no apparent break or non-linearity that might be expected if upper and lower profiles were integrating different source areas with different flux properties (Yepez et al., 2003). Air was likely well mixed within the canopy.

Despite the concerns of spatial scale and temporal matching between the isotope and sap flux techniques, the two approaches yielded very similar estimates of component fluxes in the present study for the midday period (10:30–12:30 h) between DOY 308 and 313 after irrigation (Fig. 10). Ecosystem-level transpiration and soil evaporation estimated by the isotope approach were within 4 and 15% of that estimated by scaled sap flow, respectively. These slight differences may have been due to errors in matching source areas of water vapor and isotope concentrations with eddy fluxes (Schmid, 1994; Rannik et al., 2000). Regardless, soil evaporation rates estimated by both approaches were highly correlated with vapor pressure deficit (D), as is expected for the first, energy-limited stage of soil evaporation (Ritchie, 1972). However, as with the transpiration rates estimated from sap flow, transpiration rates partitioned from total ET using the isotope technique were not correlated with D . Apparently olive trees at the south tower site at midday were transpiring at near-maximum rates set by soil and/or plant hydraulic limitations (Sperry, 2000), and thus were not sensitive to day-to-day variation in maximum D . Other studies have noted that olive is insensitive to high afternoon D (Fernández et al., 2001).

The isotope and sap flow techniques for partitioning ecosystem ET did not compare favorably for the late-afternoon sampling periods (Fig. 10). Plant transpiration declined substantially during the 2 h sampling period in the late afternoon due to

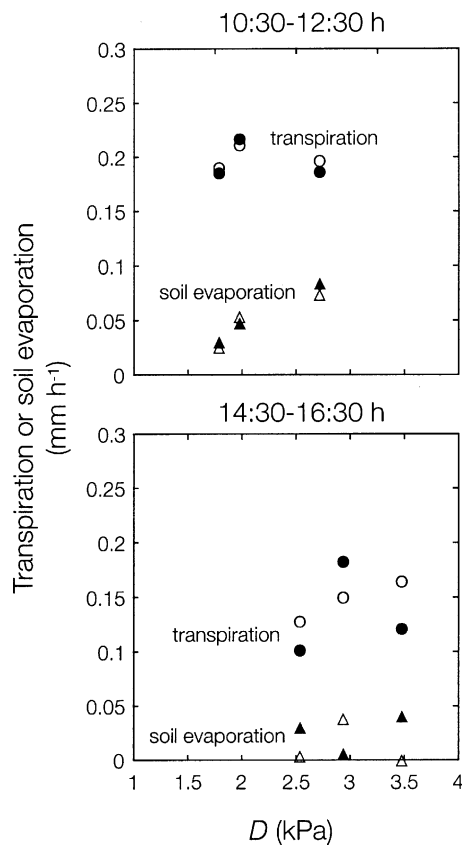


Fig. 10. Comparisons of soil evaporation and tree transpiration rates estimated from stable isotopes (solid symbols) and scaled sap flow (open symbols) plotted as a function of atmospheric vapor pressure-deficit (D).

the rapidly changing light conditions and/or high D (Figs. 2 and 7). Transpiration possibly was not at isotopic steady-state under these dynamic environmental conditions, although we have no direct evidence to support this claim. Another possible reason for the difference between isotope and sap flow partitioning for the late afternoon sampling periods is that the source area for eddy covariance fluxes and isotope concentration measurements are different. The concentration footprint and the flux footprint source areas have different decay functions in the upwind direction (Rannik et al., 2000); sources farther upwind have a greater influence on the isotope measurement than on the flux measurement. Afternoon winds were from the northwest, while in the morning winds were from the east. In the morning the upwind distance to the

non-irrigated portion of the stand to the north of the mast was much larger than in the afternoon, therefore, in the afternoon the influence of the non-irrigated section may have influenced the isotope results.

4. Summary

A greater understanding of processes driving the dynamics of soil evaporation and plant transpiration during wetting–drying episodes in arid and semiarid environments is needed to manage scarce water supplies and to elucidate factors controlling variability in ecosystem productivity. Our data illustrate the utility of the isotope ‘Keeling plot’ approach for partitioning ET at the ecosystem scale on short time steps, and the importance of accurate spatial representation of scaled sap flux for comparison with eddy covariance measurements of ET. Estimates of component ET fluxes derived by partitioning total ET using either scaled sap flow or the isotope approach were very similar for midday periods when ecosystem gas exchange was at maximum daily rates, but compared less favorably during late afternoon periods. The isotope approach, when combined with eddy covariance estimates of total ET fluxes, can be a very useful alternative to approaches that rely on scaling-up from leaf-, plant-, or plot-level measurements in heterogeneous ecosystems typical of arid and semiarid environments.

Acknowledgements

We are indebted to Drs. A. Qatibi, L. Hanich, A. Outzourhit, A. Benkaddour for use of laboratory space and equipment in Marrakech. We thank the director and staff of the Agdal olive orchard for access and use of the field site and for assistance with irrigation scheduling and security. Dr. W. Meijninger very kindly provided assistance with calculations of flux footprints. We are grateful to the Institut de Recherche pour le Développement (IRD), the University of Arizona, SAHRA-NSF Science and Technology Center, and the Dutch Science Foundation for financial support of this research. D.G. Williams was supported by a Fulbright Research Fellowship in France, E.A. Yopez was supported by a graduate research fellowship from CONACYT, Mexico, and J.C.B.

Hoedjes and O.K. Hartogensis were supported by a fellowship from STW, The Netherlands (project no. WMO3544).

References

- Aguiar, M.R., Paruelo, J.M., Sala, O.E., Lauenroth, W.K., 1996. Ecosystem responses to changes in plant functional type composition: an example from the Patagonian steppe. *J. Vegetat. Sci.* 7, 318–390.
- Allison, G.B., Barnes, C.J., Hughes, M.W., 1983. The distribution of deuterium and ^{18}O in dry soils 2. *Exp. J. Hydrol.* 64, 377–379.
- Barrett, D.J., Hatton, T.J., Nash, J.E., Ball, M.C., 1995. Evaluation of the heat pulse velocity technique for measurement of sap flow in rainforest and eucalypt forest species of southeastern Australia. *Plant Cell Environ.* 18, 463–469.
- Boulet, G., Chehbouni, A., Braud, I., Vauclin, M., Haverkamp, R., Zimmit, C., 2000. A simple water and energy balance model designed for regionalization and remote sensing data utilization. *Agric. Forest Meteorol.* 105, 117–132.
- Braud, I., Dantas-Antonino, A.C., Vauclin, M., Thony, J.L., Ruelle, P., 1995. A simple soil-plant-atmosphere transfer model (SiSPAT) development and field verification. *J. Hydrol.* 166, 213–250.
- Burgess, S.S.O., Adams, M.A., Turner, N.C., Beverly, C.R., Ong, C.K., Khan, A.A.H., Bleby, T.M., 2001. An improved heat pulse method to measure slow and reverse flow in woody plants. *Tree Physiol.* 21, 589–598.
- Burgess, S.S.O., Adams, M.A., Turner, N.C., Ong, C.K., 1998. The redistribution of soil water by tree root systems. *Oecologia* 115, 306–311.
- Craig, H., Gordon, L.I., 1965. Deuterium and oxygen-18 variations in the ocean and marine atmosphere. In: Tongiorgi, E. (Ed.) *Proceedings of the conference on stable isotopes in oceanographic studies and paleotemperatures*, Laboratory of Geology and Nuclear Science, Pisa, pp. 9–130.
- Dawson, T.E., Ehleringer, J.R., 1991. Streamside trees that do not use stream water. *Nature* 350, 335–337.
- Ehleringer, J.R., Osmond, C.B., 1989. Stable isotopes. In: Pearcy, R.W., Ehleringer, J., Mooney, H.A., Rundel, P.W. (Eds.), *Plant Physiological Ecology: Field Methods and Instrumentation*. Chapman & Hall, London, pp. 281–300.
- Evans, D.D., Sammis, T.W., Cable, D.R., 1981. Actual evapotranspiration under desert conditions. In: Evans, D.D., Thames, J.L. (Eds.), *Water in Desert Ecosystems*. Dowden, Hutchinson and Ross, Stroudsburg, PA, pp. 195–218.
- Fernández, J.E., Palomo, M.J., Díaz-Espejo, A., Clothier, B.E., Green, S.R., Girón, I.F., Moreno, F., 2001. Heat-pulse measurements of sap flow in olives for automating irrigation: tests, root flow and diagnostics of water stress. *Agric. Water Manage.* 51, 99–123.
- Ferretti, D.F., Pendall, E., Morgan, J.A., Nelson, J.A., LeCain, D., Mosier, A.R., 2003. Partitioning evapotranspiration fluxes from a Colorado grassland using stable isotopes: seasonal variations and ecosystem implications of elevated atmospheric CO_2 . *Plant Soil* 254, 291–303.
- Flanagan, L.B., Comstock, J.P., Ehleringer, J.R., 1991. Comparison of modeled and observed environmental influences on the stable oxygen and hydrogen isotope composition of leaf water in *Phaseolus vulgaris* L. *Plant Physiol.* 96, 588–596.
- Goldstein, G., Andrade, J.L., Meinzer, F.C., Holbrook, N.M., Cavelier, J., Jackson, P., Celis, A., 1998. Stem water storage and diurnal patterns of water use in tropical forest canopy trees. *Plant Cell Environ.* 21, 397–406.
- Harwood, K.G., Gillon, J.S., Roberts, A., Griffiths, H., 1999. Determinants of isotopic coupling of CO_2 and water vapour within a *Quercus petraea* forest canopy. *Oecologia* 119, 109–119.
- Helliker, B.R., Roden, J.S., Cook, C., Ehleringer, J.R., 2002. A rapid and precise method for sampling and determining the oxygen isotope ratio of atmospheric water vapor. *Rapid Commun. Mass Spectrom.* 16, 929–932.
- Horst, T.W., 1999. The footprint for estimation of atmosphere-surface exchange fluxes by profile techniques. *Boundary-Layer Meteorol.* 90, 171–188.
- Horst, T.W., Weil, J.C., 1992. Footprint estimation for scalar flux measurements in the atmospheric surface layer. *Boundary-Layer Meteorol.* 59, 279–296.
- Horst, T.W., Weil, J.C., 1994. How far is far enough? The fetch requirements for micrometeorological measurement of surface fluxes. *J. Atmos. Ocean. Tech.* 11, 1018–1025.
- Hultine, K.H., Williams, D.G., Burgess, S.S.O., Keefer, T.O., 2003. Contrasting patterns of hydraulic redistribution in three desert phreatophytes. *Oecologia* 135, 167–175.
- Hutley, L.B., O'Grady, A.P., Eamus, D., 2001. Monsoonal influences on evapotranspiration of savanna vegetation of northern Australia. *Oecologia* 126, 434–443.
- Huxman, T.E., Cable, J.M., Ignace, D.D., Eilts, J.A., English, N.B., Weltzin, J., Williams, D.G., 2004. Response of whole-ecosystem and component CO_2 and H_2O exchange to an irrigation pulse in a semi-arid grassland: contrasting geomorphic surfaces and native/non-native species communities. *Oecologia* doi: 10.1007/S00442-03-1389Y.
- Keeling, C.D., 1958. The concentration and isotopic abundance of atmospheric carbon dioxide in rural areas. *Geochim. Cosmochim. Acta* 13, 322–334.
- Kemp, P.R., Reynolds, J.F., Pachepsky, Y., Chen, J., 1997. A comparative modeling study of soil water dynamics in a desert ecosystem. *Water Resources Res.* 33, 73–90.
- Law, B.E., Falge, E., Gu, L., Baldocchi, D.D., Bakwin, P., Berbigier, P., Davis, K., Dolman, A.J., Falk, M., Fuentes, J.D., Goldstein, A., Granier, A., Grelle, A., Hollinger, D., Janssens, I.A., Jarvis, P., Jensen, N.O., Katul, G., Mahli, Y., Matteucci, G., Meyers, T., Monson, R., Munger, W., Oechel, W., Olson, R., Pilegaard, K., Paw U, K.T., Thorgeirsson, H., Valentini, R., Verma, S., Vesala, T., Wilson, K., Wofsy, S., 2002. Environmental controls over carbon dioxide and water vapor exchange of terrestrial vegetation. *Agric. Forest Meteorol.* 113, 97–120.
- MacMahon, J.A., Schimpf, D.J., 1981. Water as a factor in the biology of North American desert plants. In: Evans, D.D.,

- Thames, J.L. (Eds.), *Water in Desert Ecosystems*. Dowden, Hutchinson and Ross, Stroudsburg, PA, pp. 114–171.
- Mackay, D.S., Ahl, D.E., Ewers, B.E., Gower, S.T., Burrows, S.N., Samanta, S., Davis, K.J., 2002. Effects of aggregated classifications of forest composition on estimates of evapotranspiration in a northern Wisconsin forest. *Global Change Biol.* 8, 1253–1265.
- Majoube, M., 1971. Fractionnement en oxygène-18 et en deutérium entre l'eau et sa vapeur. *J. Chim. Phys.* 68, 1423–1436.
- Merlivat, L., 1978. Molecular diffusivities of $H_2^{18}O$ in gases. *J. Chem. Phys.* 69, 2864–2871.
- Meijninger, W.M.L., Hartogensis, O.K., Kohsiek, W., Hoedjes, J.C.B., Zuurbier, R.M., De Bruin, H.A.R., 2002. Determination of area-averaged sensible heat fluxes with a large aperture scintillometer over a heterogeneous surface–field experiment. *Boundary-Layer Meteorol.* 105, 37–62.
- Moncrieff, J.B., Jarvis, P.G., Valentini, R., 2000. Canopy fluxes. In: Sala, O.E., Jackson, R.B., Mooney, H.A., Howarth, R.W. (Eds.), *Methods in Ecosystem Science*. Springer-Verlag, New York, pp. 161–180.
- Moreira, M.Z., Sternberg, L.da S.L., Martinelli, L.A., Victoria, R.L., Barbosa, E.M., Bonates, L.C.M., Nepstad, D.C., 1997. Contribution of transpiration to forest ambient vapour based on isotopic measurements. *Global Change Biol.* 3, 439–450.
- Nelson, S.T., Dettman, D., 2001. Improving hydrogen isotope ratio measurements for on-line chromium reduction systems. *Rapid Commun. Mass Spectrom.* 15, 2301–2306.
- Noy-Meir, I., 1973. Desert ecosystems: environment and producers. *Annu. Rev. Ecol. Syst.* 4, 51–58.
- Paruelo, J.M., Sala, O.E., 1995. Water losses in the Patagonian steppe: a modelling approach. *Ecology* 76, 510–520.
- Phillips, D.L., Gregg, J.W., 2001. Uncertainty in source partitioning using stable isotopes. *Oecologia* 127, 171–179.
- Prince, S.D., Brown de Colstoun, E., Kravitz, L.L., 1998. Evidence from rain-use efficiencies does not indicate extensive Sahelian desertification. *Global Change Biol.* 4, 359–374.
- Rannik, Ü., Aubinet, M., Kurbanmuradov, O., Sabelfeld, K.K., Markkanen, T., Vesala, T., 2000. Footprint analysis for measurements over a heterogeneous forest. *Boundary-Layer Meteorol.* 97, 137–166.
- Reynolds, J.F., Kemp, P.R., Tenhunen, J.D., 2000. Effects of long-term rainfall variability on evapotranspiration and soil water distribution in the Chihuahuan desert: a modeling analysis. *Plant Ecol.* 150, 145–159.
- Ritchie, J.T., 1972. Model for predicting evaporation from a row crop with incomplete cover. *Water Resources Res.* 8, 1204–1213.
- Sammis, T.W., Gay, L.Y., 1979. Evapotranspiration from an arid zone plant community. *J. Arid Environ.* 2, 313–321.
- Scott, R.L., Watts, C., Garatuza, J., Edwards, E., Goodrich, D.C., Williams, D.G., Shuttleworth, W.J., 2003. The understory and overstory partitioning of energy and water fluxes in a semi-arid woodland ecosystem. *Agric. Forest Meteorol.* 114, 127–139.
- Schaeffer, S.M., Williams, D.G., Goodrich, D.C., 2000. Transpiration in cottonwood/willow forest patches estimated from sap flux. *Agric. Forest Meteorol.* 105, 257–270.
- Schmid, H.P., 1994. Source areas for scalars and scalar fluxes. *Boundary-Layer Meteorol.* 67, 293–318.
- Smith, S.D., Herr, C.A., Leary, K.L., Piorkowsky, J.M., 1995. Soil-plant water relations in a Mojave desert mixed shrub community: a comparison of three geomorphic surfaces. *J. Arid Environ.* 29, 339–351.
- Sperry, J.S., 2000. Hydraulic limits on plant gas exchange. *Agric. Forest Meteorol.* 104, 13–23.
- Swanson, R.H., 1994. Significant historical developments in thermal methods for measuring sap flow in trees. *Agric. Forest Meteorol.* 72, 113–132.
- Swanson, R.H., Whitfield, D.W.A., 1981. A numerical analysis of heat pulse velocity and theory. *J. Exp. Bot.* 32, 221–239.
- Thornburn, P.J., Walker, G.R., Brunel, J.-P., 1993. Extraction of water from eucalyptus trees for analysis of deuterium and oxygen-18: laboratory and field techniques. *Plant Cell Environ.* 16, 269–277.
- Wang, X.F., Yakir, D., 1995. Temporal and spatial variations in oxygen-18 content of leaf water in different plant species. *Plant Cell Environ.* 18, 1377–1385.
- Wang, X.F., Yakir, D., 2000. Using stable isotopes of water in evaporation studies. *Hydrol. Process.* 14, 1407–1421.
- Webb, E.K., Pearman, G.I., Leuning, R., 1980. Correction of flux measurements for density effects due to heat and water vapor transfer. *Q. J. R. Meteor. Soc.* 106, 85–100.
- Williams, D.G., Ehleringer, J.R., 2000. Intra- and interspecific variation for summer precipitation use in pinyon-juniper woodlands. *Ecol. Monogr.* 70, 517–537.
- Wilson, K.B., Hanson, P.J., Mulholland, P.J., Baldocchi, D.D., Wullschlegel, S.D., 2001. A comparison of methods for determining forest evapotranspiration and its components: sap-flow, soil water budget, eddy covariance and catchment water balance. *Agric. Forest Meteorol.* 106, 153–168.
- Yakir, D., Sternberg, L. da S.L., 2000. The use of stable isotopes to study ecosystem gas exchange. *Oecologia* 123, 297–311.
- Yepez, E.A., Williams, D.G., Scott, R., Lin, G., 2003. Partitioning overstory and understory evapotranspiration in a semi-arid savanna ecosystem from the isotopic composition of water vapor. *Agric. Forest Meteorol.* 119, 53–68.